J Mater Sci (2016) 51:2935–2941
DOI 10.1007/s10853-015-9602-z

Artificial honeycomb-inspired TiO_2 nanorod arrays with tunable nano/micro interfaces for improving poly(dimethylsiloxane) surface hydrophobicity

Rongxiang He[1] · Jingrong Xiao[1] · Minli Zhang[1] · Zhengtao Zhang[1] · Weiying Zhang[1] · Yiping Cao[1] · Yumin Liu[1] · Yong Chen[1,2]

Received: 15 October 2015 / Accepted: 16 November 2015 / Published online: 7 December 2015

Abstract This work demonstrates a bottom-up model of fabricating a honeycomb-inspired interface consisting of micro- and nanostructures for improving poly(dimethylsiloxane) (PDMS) hydrophobicity. TiO_2 nanorod arrays and microsized voids were fabricated by a two-step hydrothermal reaction method. First, rutile TiO_2 nanorod arrays were hydrothermally fabricated on the fluorine-doped SnO_2 conductive substrates substrate. Second, microsized TiO_2 voids were synthesized through HCl hydrothermal etching to obtain a honeycomb-inspired interface with tunable size. The size of the etched voids increased from 0.22 ± 0.06 to 8.0 ± 2.8 μm. The interfaces were then transferred on the PDMS surface to improve hydrophobic property. The contact angles of the corresponding positive PDMS replicas reached 140° after etching with the TiO_2 nanorod arrays for 10 h. The size of mastoid structures on the PDMS surfaces was 7.5 μm, which is similar to the size of microstructures on the lotus leaf surface. The fabricated PDMS surface with tunable hydrophobicity properties can be used in the microfluidic channels in the future.

Jingrong Xiao and Minli Zhang have contributed equally to this work.

Electronic supplementary material The online version of this article (doi:10.1007/s10853-015-9602-z) contains supplementary material, which is available to authorized users.

✉ Rongxiang He
herx@jhun.edu.cn

✉ Yumin Liu
ymliu@jhun.edu.cn

✉ Yong Chen
yong.chen@ens.fr

[1] Institute for Interdisciplinary Research & Key Laboratory of Optoelectronic Chemical Materials and Devices, Ministry of Education, Jianghan University, Wuhan 430056, China

[2] Département de Chimie, Ecole Normale Supérieure, 24 Rue Lhomond, 75231 Paris Cedex05, France

Introduction

Wettability plays a significant function in our daily lives, such as self-clean phenomenon, and the surface-wetting property of solid materials is determined by their chemical components and surface geometrical morphology [1, 2]. Plant leaves exhibit excellent superhydrophobic surface characteristics, allowing dust or debris particles to easily roll off and be carried away by water droplets on the leaf surface—this phenomenon is known as self-cleaning [3, 4]. The crucial determining factors of this mechanism are surface micro/nanoscale papillae and epicuticular wax [5]. Inspired by the mechanical and configurable nature characteristics, such as the structures on the surface of rose petals [6] and lotus leaf [5], researchers have developed various methods for fabricating biomimetic materials and structures [7–9]. Artificial biomimetic functional materials with the micro/nanosurface morphologies, which exhibit special wettability characteristics have attracted much attention [1], for superhydrophilic, superhydrophobic [10], and oil–water separation. Based on the self-cleaning phenomenon, these micro/nanostructure interfaces can also be used for anti-bacteria and anti-fogging applications [11].

Controlling the bio-interface between substrate and biosamples is important in the biomedical detection and diagnosis. In our previous work, TiO_2 nanofiber or

nanoparticles and MnO_2 nanoparticles on the flat substrate were utilized to capture rare circulating tumor cells in human peripheral blood [12–14], with dominant nanostructure characteristics on the cancer cell surface. In another study, the poly(dimethylsiloxane) (PDMS) micropillars were used as substrate for capturing cancer cells, with dominant characteristic of the microsized cells [15]. However, these methods present certain limitations, such as utilization of only one characteristic of cancer cells, namely, nanostructure or cell size. Therefore, an interface that consists of nano/micro-sized structure must be developed [16].

Bio-inspired interfaces are fabricated using various methods, such as nanoimprinting [17], point-by-point femto second laser scanning process [18], reactive-ion etching [19], and electrospinning [9]. In this work, we introduce a bottom-up model to fabricate a honeycomb-inspired interface consisting of micro/nanostructures. First, TiO_2 nanorod arrays (NRAs) were fabricated on the substrate by the hydrothermal method. Second, the surface was processed by chemical etching to generate microsized structures without any photomask. The size of these structures can be controlled by adjusting chemical etching duration. In particular, the size of the etched voids was increased from 0.22 ± 0.06 to 8.0 ± 2.8 μm. The nano/microstructures were then transferred onto the PDMS surface to control the water wettability. The contact angles (CA) of positive and negative PDMS replicas were further investigated. The CA of the replicas increased from 108° on the flat condition to 140° on the nano/microstructure condition. These results can be utilized to partly explain why the nature selects large-sized papillae on a lotus leaf.

Materials and methods

Materials

Fluorine-doped SnO_2-conductive substrates (FTO, 2.8 cm × 5.0 cm, sheet resistance 10–15 $\Omega\ sq^{-1}$) were purchased from Asahi Glass, Japan. Acetone, ethanol, $TiCl_4$, and HCl were acquired from Sinopharm Chemical Reagent Co., Ltd, China. PDMS (RTV615) was obtained from Momentive, USA. Deionized (DI) water was generated from a MILLI-Q system (Millipore, MA, USA). All reagents were used without additional treatment. A 0.2 M TiCl4 pretreatment aqueous solution was prepared by slowly adding 3 mL of $TiCl_4$ into a mixture containing 95 mL of DI water and 2 mL of concentrated HCl under magnetic stirring for 30 min. A TiO_2 growth solution was prepared by adding 3 mL of $TiCl_4$ dropwise to a mixture containing 30 mL of DI water and 30 mL of concentrated HCl under stirring for 3 h.

Synthesis of highly oriented rutile TiO_2 NRAs

Highly oriented rutile TiO_2 NRAs were synthesized on conductive substrate via hydrothermal process, according to previous research [20–23]. FTO glasses were sequentially ultrasonically cleaned in acetone, ethanol, and DI water, and then immersed to 0.2 M $TiCl_4$ aqueous solution at 70 °C for 40 min to deposit TiO_2 germ crystals. After washing three times with DI water, $TiCl_4$ treated FTO substrates were annealed in air at 550 °C for 1 h, ultrasonically washed three times with DI water, and then dried. The treated FTO glasses with conductive sides facing down were added with 63 mL of $TiCl_4$ growth aqueous and immobilized on polytef-lined stainless hydrothermal reactors. The reactors were then placed in a forced-air convection drying oven for 12 h at 150 °C. The as-prepared TiO_2 NRAs on the FTO glasses were washed three times with DI water and dried.

Microsized voids etched by HCl

The as-prepared highly ordered rutile TiO_2 NRAs were chemically etched in a solution of 40 mL of concentrated HCl and 20 mL of DI water at 150 °C for different durations to obtain microsized void structures. The substrates were then washed three times with DI water and dried [20]. This two-step hydrothermal reaction enabled the production of a nano/micro interface.

Fabrication of PDMS replica with nano/micro interface

A PDMS prepolymer mixture (base monomer: cross linker = 9:1) was poured onto TiO_2 NRAs. After degassing, the PDMS was cured in an oven at 80 °C for 3 h, peeled, and then used as negative templates. The surface of the negative PDMS template was treated by oxygen plasma for 90 s to obtain a positive replica. The PDMS prepolymer mixture (base monomer: cross linker = 10:1) was poured onto the negative template, cured and then peeled to obtain a positive replica. The employed transfer method has been discussed in the literature [24–27].

Characterization

The surface morphology of the highly aligned TiO_2 NRAs as well as the negative and the positive PDMS replicas was characterized through ultrahigh-resolution cold field scanning electron microscopy (SU8010, HITACHI, Japan). X-ray diffraction (XRD) patterns of the TiO_2 film before and after etched by HCl were performed on a PANalytical XRD system (X'Pert Powder) with Cu $K\alpha$ radiation ($\lambda = 1.54056$ Å). The water CAs of the PDMS replica

samples were measured using an optical CA instrument (JC2000C1, Shanghai Zhongchen Digital Technology Apparatus Co.Ltd, China) at ambient temperature with 2 μL DI of water droplet. The CAs from three positions were measured and then averaged.

Results and discussion

Honeycomb-inspired TiO_2 NRAs interface fabrication

We propose a bottom-up model for fabricating a honeycomb-inspired interface consisting of micro/nano structures. A nanosized structure was synthesized on the FTO substrate. As illustrated in steps 1 and 2 in Fig. 1, highly ordered aligned rutile TiO_2 NRAs were hydrothermally grown on the FTO substrate. These NRAs are used as photoanode in dye-sensitized solar cells because of their optoelectronic properties [20, 28, 29]. The length and film thickness of TiO_2 NRAs were affected by hydrothermal reaction time. A previous work indicated that film thickness rapidly increased as the hydrothermal reaction time increased from 3 h to 30 h and then remained stable; this finding could be due to rapid Ti^{4+} hydrolysis over the precursors [20]. In the present work, we used the nanostructure as basic substrate and preformed the hydrothermal growth treatment for 12 h, as shown in step 2 in Fig. 1. The cross-sectional and surface morphologies of the scanning electron microscope (SEM) images are shown in Fig. S1a and b, respectively. The thickness of the as-prepared unetched NRAs was about 24 μm.

Microsized voids on the TiO_2 NRA surfaces were generated through hydrothermal chemical etching, as shown in step 3 in Fig. 1. Void size was affected by the etching time during the hydrothermal reaction (Fig. 2). The etching times in Fig. 2a–h were 0, 1, 2, 3, 4, 7, 10, and 14 h, respectively. The dash line in Fig. 2h illustrates a void. After etching, the rutile nanorods contained continuous aggregated small TiO_2 nanorods [23], as shown in Fig. S2. XRD patterns of TiO_2 NRAs before and after etched by HCl are shown in Fig. S3, which indicated that the HCl hydrothermal reaction process did not change the rutile structures. The fabricated TiO_2 NRAs were bonded on the top. Figure 2 indicates that void size increased with the increasing etching time. The void size of the as-prepared TiO_2 NRAs was about 0.26 μm and increased to 3.9 ± 1.6 μm, when the etching time was increased to 3 h. Moreover, the void size increased to 8.0 ± 2.8 μm when the etching time was further increased to 10 h. The relationships between the size and height of voids and the hydrothermal etching time are shown in Fig. 3. The average height increased from 0.7 to 10.7 μm when the etching time was increased from 1 to 10 h, which could be attributed to the formation of secondary TiO_2 nano crystalline on the nanorods [29–31].

PDMS negative and positive replica

Nano/microsized structures were transferred on the PDMS surface to enhance hydrophobic characteristics. PDMS is a polymer elastomer widely used in microfluidic systems and for nanocasting, because this material features hydrophobicity, flexibility, transparency, and fast curing. Negative PDMS replicas were fabricated (steps 4 and 5 in Fig. 1) and used as templates to fabricate positive PDMS replicas (steps 6 and 7 in Fig. 1). The positive PDMS replicas corresponding to TiO_2 NRAs with etching times of 0–14 h

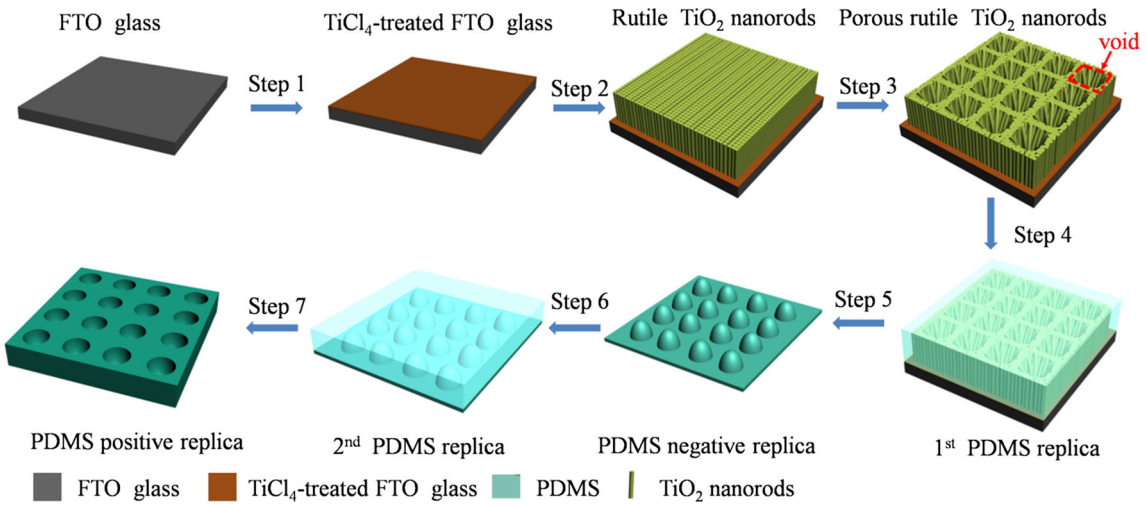

Fig. 1 Illustration of the fabrication of nano/microsized TiO_2 NRAs by means of a two-step hydrothermal synthesis method (steps1–3) and the syntheses of the negative and the positive PDMS replicas (steps 4–7)

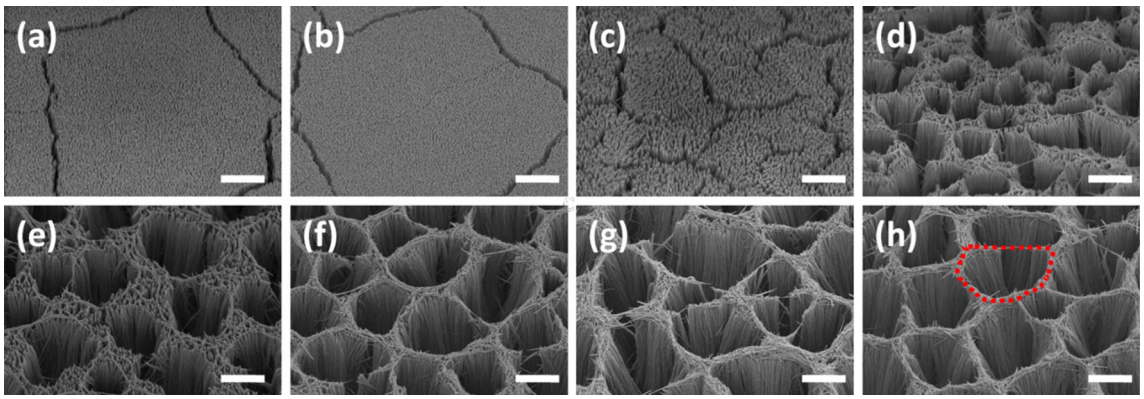

Fig. 2 Top view of SEM images of TiO_2 NRAs etched by HCl at different durations. **a** 0, **b** 1, **c** 2, **d** 3, **e** 4, **f** 7, **g** 10, and **h** 14 h. The *scale bars* are all 4 μm. The *dashed line* in (h) presents a void after hydrothermal chemical etching

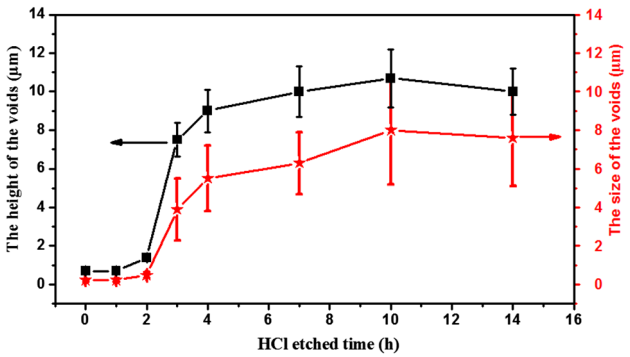

Fig. 3 The change of size and height of the etched voids as a function of etching time

are shown in Fig. 4a–h. The surface morphologies of these nanorods exhibited increased roughness with the increasing etching time. Minimal changes occurred on the PDMS surface after twice replicas: because PDMS is hydrophobic and TiO_2 is hydrophilic. The enlarged SEM images (Fig. S4) of the positive PDMS replica etched for 4 h showed the presence of many nano/microsized structures. The surface morphology derived from the SEM images of the negative PDMS replicas is shown in Fig. S5. The size of the mastoid structures increased with the increasing time, and this finding is consistent with that on void size. The enlarged SEM images (Fig. S6) of the negative PDMS replica etched for 10 h showed a single papilla-like structure.

The cross-sectional morphology SEM images of the TiO_2 NRAs and their corresponding positive PDMS replicas are shown in Fig. 5. The etching times as shown in Fig. 5a–d were 1, 4, 7, and 10 h, respectively. The height of the microscale mastoid structures on the PDMS surfaces gradually increased with the increasing etching time. The average height of the PDMS mastoid structures reached the highest value of 7.5 μm when the etching time was 10 h. The obtained height was smaller than the corresponding height of the voids, which could be attributed to the fact that the PDMS surface is hydrophobic and the TiO_2 surface is hydrophilic. Therefore, during the formation of PDMS replicas, the mixed PDMS prepolymer cannot fulfill the voids, particularly the nanosized bottom.

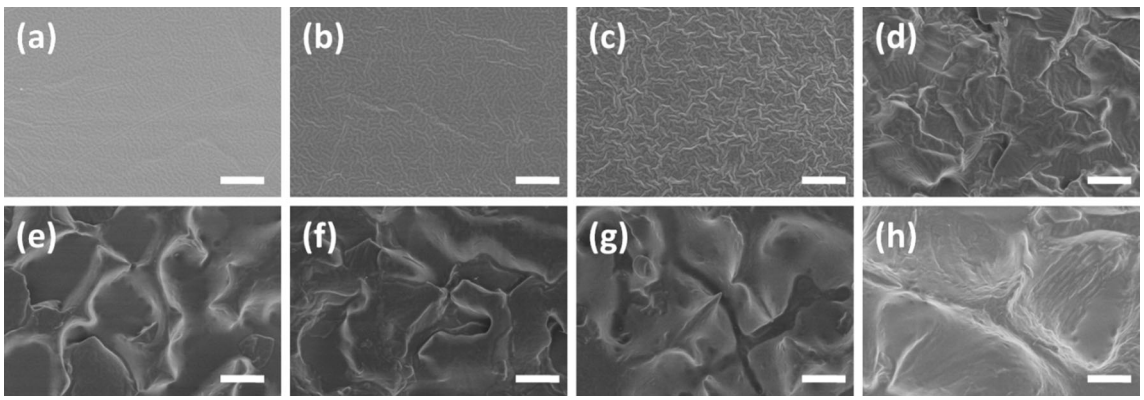

Fig. 4 SEM images of the positive PDMS replica. **a–h** TiO_2 NRA templates hydrothermally etched at 0, 1, 2, 3, 4, 7, 10, and 14 h, respectively. All *scale bars* are 4 μm

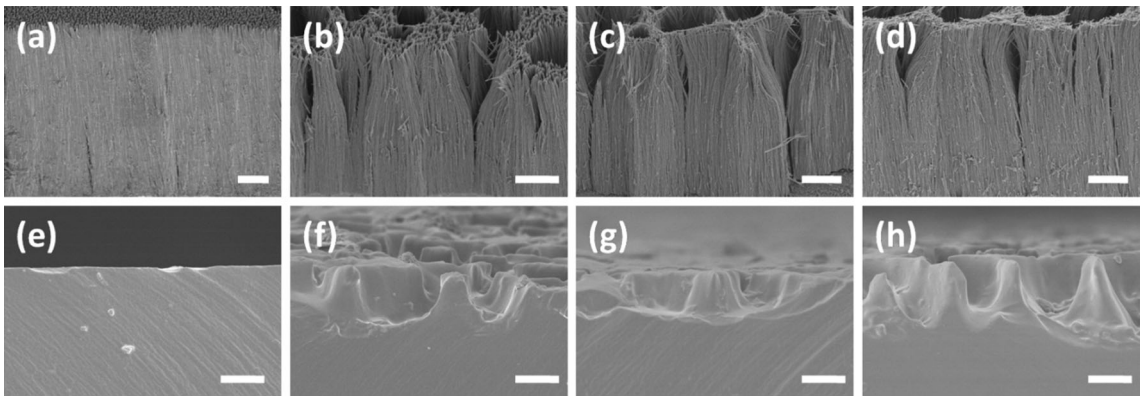

Fig. 5 Cross-sectional SEM images of TiO_2 NRAs etched at different time. **a** 1, **b** 4, **c** 7, and **d** 10 h, respectively. **e**–**h** Positive PDMS replicas corresponding to (**a**–**d**). All *scale bars* are 4 μm

CAs of PDMS replicas characterization

Wetting is an important characteristic of solid surfaces and determined by the chemical composition and surface morphology of the material. In this study, 2 μL of DI water droplets were introduced on the nano/microsized interfaces to investigate the hydrophobicity properties of negative and positive PDMS replicas. CA was measured on three different positions on each replica. As shown in Fig. 6, the CA of flat PDMS, which was used as the control sample, was about 108°. The CA of the positive PDMS replicas was higher than that of the flat PDMS at etching times lower than 3 h. The CA of the corresponding positive PDMS replicas was about 140°, which increased by 30 % compared to that of the flat PDMS, when the etching time was about 10 h. Moreover, the CA was about 115° at etching times of 0, 1, and 2 h. This result is similar to that of SWA PDMS replicated using the nanoporous anodic aluminum oxide template [32]; the sizes of the structures on the positive PDMS replicas were <1 μm. The sizes of mastoid structures on the PDMS surfaces increased to 7.5 μm, when the etching time was about 10 h; this finding is similar to that on microstructures on the lotus leaf surface (SEM images of the negative and positive PDMS replicas are shown in Fig. S7.). Overall, CA increased with the increasing sizes of the mastoid structures and differed between positive and negative PDMS samples replicated by the lotus leaf [3]. The CAs of the positive and negative PDMS replicas were about 160° and 110°, respectively [3], which are similar to those of the samples replicated by the etched TiO_2 NRAs because similar nano/microsized structures existed on the surface.

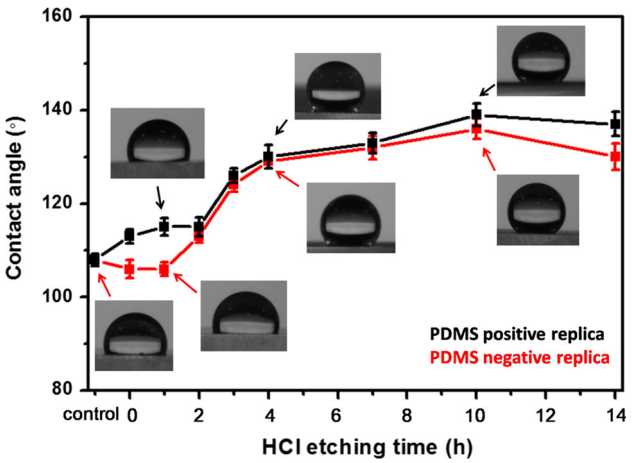

Fig. 6 Contact angles of the positive and the negative PDMS replicas replicated by the TiO_2 NRA etching at different times from 0 to 14 h. The photographs of the water droplet on some replicas are also shown

Conclusion

A bottom-up model is proposed to fabricate a honeycomb-inspired interface consisting of micro/nanostructures for improving PDMS hydrophobicity. A two-step hydrothermal reaction was used to synthesize TiO_2 NRAs and microsized voids. Void size can be controlled by manipulating HCl hydrothermal etching time. As such, the size of the etched voids can be increased from 0.22 ± 0.06 to 8.0 ± 2.8 μm, which is similar to the size of the nanoscale microvilli on cancer cell surfaces and to the size of cancer cells [33]. We also investigated the effect of the nano/microsized interface on the hydrophobicity properties of the PDMS surface. The CAs of the corresponding positive and negative PDMS replicas slightly increased from 108° to 115° when the etching time of TiO_2 NRAs was less than 3 h. The CA also reached about 140° which increased by 30 % compared to that of the flat PDMS, when the etching time was about 10 h. Under this condition, the size of

mastoid structures on the PDMS surface was about 7.5 μm, which is similar to the size of microstructures on the lotus leaf surface. Therefore, this nano/microsized interface can be used to obtain tunable hydrophobic PDMS surface without any chemical modification. The fabricated surface can be used to improve the interface between the liquid and PDMS surface in microfluidic channels.

Acknowledgements This work was financial supported by the National Natural Science Foundation of China (Grant Nos. 81402466, 61404060) and the Natural Science Foundation of Hubei (No. 2015CFB610). The authors also acknowledge the financial support from the Ph.D. research foundation of Jianghan University.

Compliance with ethical standards

Conflict of interest The authors declare that they have no conflict of interest.

References

1. Sun TL, Feng L, Gao XF, Jiang L (2005) Bioinspired surfaces with special wettability. Acc Chem Res 38:644–652
2. Jin MH, Feng XJ, Xi JM, Zhai J, Cho K, Feng L, Jiang L (2005) Super-hydrophobic PDMS surface with ultra-low adhesive force. Macromol Rapid Commun 26:1805–1809
3. Sun MH, Luo CX, Xu LP, Ji H, Ouyang Q, Yu DP, Chen Y (2005) Artificial lotus leaf by nanocasting. Langmuir 21:8978–8981
4. Su B, Li M, Lu QH (2010) Toward understanding whether superhydrophobic surfaces can really decrease fluidic friction drag. Langmuir 26:6048–6052
5. Feng L, Li S, Li Y, Li H, Zhang L, Zhai J, Song Y, Liu B, Jiang L, Zhu D (2002) Super-hydrophobic surfaces: from natural to artificial. Adv Mater 14:1857–1860
6. Chou SY, Yu CC, Yen YT, Lin KT, Chen HL, Su WF (2015) Romantic story or raman scattering? Rose petals as ecofriendly, low-cost substrates for ultrasensitive surface-enhanced raman scattering. Anal Chem 87:6017–6024
7. Cheng QF, Jiang L, Tang ZY (2014) Bioinspired layered materials with superior mechanical performance. Acc Chem Res 47:1256–1266
8. Hou X, Guo W, Jiang L (2011) Biomimetic smart nanopores and nanochannels. Chem Soc Rev 40:2385–2401
9. Bai H, Ju J, Zheng YM, Jiang L (2012) Functional fibers with unique wettability inspired by spider silks. Adv Mater 24:2786–2791
10. Jiang L, Zhao Y, Zhai J (2004) A lotus-leaf-like superhydrophobic surface: a porous microsphere/nanofiber composite film prepared by electrohydrodynamics. Angew Chem Int Ed 116:4438–4441
11. Liu KS, Cao MY, Fujishima A, Jiang L (2014) Bio-inspired titanium dioxide materials with special wettability and their applications. Chem Rev 114:10044–10094
12. Zhang NG, Deng YL, Tai QD, Cheng BR, Zhao LB, Shen QL, He RX, Hong LY, Liu W, Guo SS, Liu K, Tseng HR, Xiong B, Zhao XZ (2012) Electrospun TiO_2 nanofiber-based cell capture assay for detecting circulating tumor cells from colorectal and gastric cancer patients. Adv Mater 24:2756–2760
13. He RX, Zhao LB, Liu YM, Zhang NG, Cheng BL, He ZB, Cai B, Li SS, Liu W, Guo SS, Chen Y, Xiong B, Zhao XZ (2013) Biocompatible TiO_2 nanoparticle-based cell immunoassay for circulating tumor cells capture and identification from cancer patients. Biomed Microdevices 15:617–626
14. Huang QQ, Chen BL, He RX, He ZB, Cai B, Xu JH, Qian WY, Chan HL, Liu W, Guo SS, Zhao XZ, Yuan JK (2014) Capture and release of cancer cells based on sacrificeable transparent MnO_2 nanospheres thin film. Adv Healthc Mater 3:1420–1425
15. Xiao JR, He WQ, Zhang ZT, Zhang WY, Cao YP, He RX, Chen Y (2015) PDMS micropillar-based microchip for efficient cancer cell capture. RSC Adv 5:52161–52166
16. Wang S, Liu K, Yao X, Jiang L (2015) Bioinspired surfaces with superwettability: new insight on theory, design, and applications. Chem Rev 115:8230–8293
17. Law JBK, Ng AMH, He AY, Low HY (2014) Bioinspired ultrahigh water pinning nanostructures. Langmuir 30:325–331
18. Yong J, Chen F, Yang Q, Zhang D, Bian H, Du G, Si J, Meng X, Hou X (2013) Controllable adhesive superhydrophobic surfaces based on PDMS microwell arrays. Langmuir 29:3274–3279
19. Oh JK, Lu X, Min Y, Cisneros-Zevallos L, Akbulut M (2015) Bacterially antiadhesive optically transparent surfaces inspired from rice leaves. ACS Appl Mater Interfaces 7:19274–19281
20. Lv M, Zheng D, Ye M, Xiao J, Guo W, Lai Y, Sun L, Lin C, Zuo J (2013) Optimized porous rutile TiO_2 nanorod arrays for enhancing the efficiency of dye-sensitized solar cells. Energy Environ Sci 6:1615–1622
21. Hwang YJ, Hahn C, Liu B, Yang P (2012) Photoelectrochemical properties of TiO_2 nanowire arrays: a study of the dependence on length and atomic layer deposition coating. ACS Nano 6:5060–5069
22. Zhang X, Liu Y, Lee ST, Yang S, Kang Z (2014) Coupling surface plasmon resonance of gold nanoparticles with slow-photon-effect of TiO_2 photonic crystals for synergistically enhanced photoelectrochemical water splitting. Energy Environ Sci 7:1409–1419
23. Liu YM, Zhang ML, Jiang Y, Xia Y, Sun WW, Zhao XZ (2015) General strategy to construct hierarchical TiO_2 nanorod arrays coupling with plasmonic resonance for dye-sensitized solar cells. Electrochim Acta 173:483–489
24. Su B, Gong S, Ma Z, Yap LW, Cheng W (2015) Mimosa-inspired design of a flexible pressure sensor with touch sensitivity. Small 11:1886–1891
25. Dey R, Raj MK, Bhandaru N, Mukherjee R, Chakraborty S (2014) Tunable hydrodynamic characteristics in microchannels with biomimetic superhydrophobic (lotus leaf replica) walls. Soft Matter 10:3451–3462
26. Liu B, He Y, Fan Y, Wang X (2006) Fabricating super-hydrophobic lotus-leaf-like surfaces through soft-lithographic imprinting. Macromol Rapid Commun 27:1859–1864
27. He WQ, Xiao JR, Zhang ZT, Zhang WY, Cao YP, He RX, Chen Y (2015) One-step electroplating 3D template with gradient height to enhance micromixing in microfluidic chips. Microfluid Nanofluid 19:829–836
28. Liu B, Aydil ES (2009) Growth of oriented single-crystalline rutile TiO_2 nanorods on transparent conducting substrates for dye-sensitized solar cells. J Am Chem Soc 131:3985–3990
29. Guo W, Xu C, Wang X, Wang S, Pan C, Lin C, Wang ZL (2012) Rectangular bunched rutile TiO_2 nanorod arrays grown on carbon fiber for dye-sensitized solar cells. J Am Chem Soc 134:4437–4441
30. Cheng H, Ma J, Zhao Z, Qi L (1995) Hydrothermal preparation of uniform nanosize rutile and anatase particles. Chem Mater 7:663–671
31. Kumar A, Madaria AR, Zhou C (2010) Growth of aligned single-crystalline rutile TiO_2 nanowires on arbitrary substrates and their application in dye-sensitized solar cells. J Phys Chem C 114:7787–7792

32. Dudem B, Ko YH, Leem JW, Lee SH, Yu JS (2015) Highly transparent and flexible triboelectric nanogenerators with sub-wavelength-architectured polydimethylsiloxane by a nanoporous anodic aluminum oxide template. ACS Appl Mater Interfaces 7:20520–20529

33. Fischer KE, Alemán BJ, Tao SL, Daniels RH, Li EM, Bünger MD, Nagaraj G, Singh P, Zettl A, Desai TA (2009) Biomimetic nanowire coatings for next generation adhesive drug delivery systems. Nano Lett 9:716–720